



Direct conversion of mouse embryonic fibroblast to osteoblast cells using hLMP-3 with Yamanaka factors

Mahmoud F. Ahmed^{a,b}, Ahmed Kamel El-Sayed^b, Hao Chen^c, Ruifeng Zhao^a, Kai Jin^a, Qisheng Zuo^a, Yani Zhang^a, Bichun Li^{a,*}

^a Key Laboratory of Animal Breeding, Reproduction and Molecular Design for Jiangsu Province, College of Animal Science and Technology, Yangzhou University, Yangzhou, 225009, China

^b College of Veterinary Medicine, Suez Canal University, Ismailia, 41522, Egypt

^c Department of Orthopedics, The First Affiliated Hospital of Soochow University, No. 188 Shizi Street, Suzhou, Jiangsu, 215006, China

ARTICLE INFO

Keywords:

MEF
hLMP-3
Yamanaka factors
Direct reprogramming
Bone regeneration

ABSTRACT

Large bone defects and bone loss after fractures remain significant challenges for orthopedic surgeons. Our study aims to find an available, applicable and biological treatment for bone regeneration overcoming the limitations in ESC/iPSC technology. We directly reprogrammed the mouse embryonic fibroblast (MEF) into osteoblast cells using different combinations of Yamanaka factors with human lim mineralization protein-3 (hLMP-3). LMP is an intracellular LIM-domain protein acting as an effective positive regulator of the osteoblast differentiation. After transduction, cells were cultured in osteogenic medium, and then examined for osteoblast formation. The expression of osteogenic markers (BMP2, Runx2 and Osterix) during reprogramming and *in vitro* mineralization assay revealed that the best reprogramming cocktail was (c-Myc – Oct4) with hLMP-3. In addition, both immunofluorescent staining and western blot analysis confirmed that osteocalcin (OCN) expression increased in the cells treated with the c-Myc/Oct4/hLMP3 cocktail than using hLMP-3 alone. Furthermore, this reprogramming cocktail showed efficient healing in an induced femoral bone defect in rat animal model one month after transplantation. In the present study, we reported for the first time the effect of combining Yamanaka factors with hLMP-3 to induce osteoblast cells from MEF both *in vitro* and *in vivo*.

1. Introduction

The regeneration of bone tissue for transplantation therapies represents a serious health problem, and still remains a significant challenge for efficient clinical interventions. This is because the available therapeutic approaches are often accompanied with prolonged treatments, pain, infection risk, hemorrhage, nerve damage, and locomotor disability. The development of new therapeutic tools for bone repair to meet these obstacles is urgent nowadays. Recently, the blossoming fields of cell therapy, and tissue engineering hold great expectations for overcoming the current roadblocks that hinder long-term, successful clinical outcomes (Caplan, 2007). The main challenge in tissue engineering is to find safer and available cell sources for isolation or generation. For example, transplantation of isolated osteoblasts is limited by inadequate cell availability, and poor survivability of transplanted cells (Park et al., 2006). In the same context, invasive procedures during harvesting MSC reduce its privilege (Hjortholm et al., 2013; Kim et al., 2011). Meanwhile, the tumorigenic risk of using ESCs

and iPSCs impedes their clinical application (Li et al., 2008; Okita and Yamanaka, 2011; Walia et al., 2012). Therefore, it's essential to develop another cell source for bone regeneration, to avoid the current drawbacks in the available cell sources (Li et al., 2016). For achieving the mile-stone of regeneration, one interesting technology is to convert differentiated cell type into another *via* transcription factors, micro-RNA or lineage specific stimulating medium or the combination of them (Ullah et al., 2014).

The development of lineage/direct reprogramming is more effective, and faster approach than iPSCs generation. The technique of direct reprogramming somatic cells into another cell lineage has major therapeutic considerations. One of these considerations is to avoid any intermediate pluripotent state, consequently, decrease the risk of tumorigenesis after cell implantation. Another one is to overcome the probability of the immunogenicity identified recently in iPSCs (Zhao et al., 2011). Overall, only a minimum invasive intervention is required to obtain large amounts of patient's own fibroblasts. This facilitates an autologous cell therapy, whenever cell replacement is required in

* Corresponding author.

E-mail address: yubcli@yzu.edu.cn (B. Li).

clinical situations (Costa-Almeida et al., 2018). Indeed several reports used the fibroblast cells for bone regeneration (Lattanzi et al., 2008; Sommar et al., 2013; Yamamoto et al., 2015, 2018).

Cell-mediated gene therapy in which genetically engineered cells used for transplantation, has a great potential to accelerate bone regeneration during treatment of orthopedic disorders (Evans et al., 2009). In addition, cell-mediated gene therapy has the advantage of controlled and efficient cell transduction in comparison with direct gene delivery. Moreover, it increases the cellularity at the recipient lesion site, allow the selection of cell source, and capitalizing on an autocrine and paracrine effect. For all these reasons, the transplanted cells have the ability to differentiate into target cell types, and in the same time secrete osteogenic mediators into the transplantation site (Ishihara, 2009).

The osteo-inductive growth factor, hLMP has a direct correlation with osteoblastic differentiation (Salgia et al., 1995), and appeared to be a positive regulator of bone formation (Minamide et al., 2003). Unlike BMPs, which are extracellular signaling molecule, and effect through cell-surface receptors, hLMPs are intracellular proteins and their therapeutic usage requires gene transfer of their cDNA into the host cells (*in vivo* gene therapy) or application of transfected carrier cells (*ex vivo* gene therapy). LMP gene transfer can induce synthesis of multiple BMPs such as: BMP2, 4, 6, 7, as well as TGF- β (Minamide et al., 2003). The main advantage of LMP is that it produces multiple osteogenetic growth factors by administration of a single therapeutic molecule (Yoon and Boden, 2004). Previous reports clearly showed the effectiveness of LMP for bone healing enhancement (Minamide et al., 2003; Pola et al., 2004), and indicate the promising application of this growth factor.

The LMP-3 splice variant, has the ability to upregulate the expression of bone-specific markers (osteocalcin, osteopontin, bone sialoprotein) in both pre-osteoblastic and non-osteoblastic cell lines. Besides, it can induce *in vitro* mineralization and *in vivo* bone formation (Pola et al., 2004). LMP-3 promoted the osteogenesis program in MSCs, calvarial osteoblasts and fibroblasts stimulated osteo-lineage differentiation *in vitro* (Boden et al., 1998, 1999; Liu et al., 2002; Pola et al., 2004). Fibroblasts transduced with AdLMP3 repaired a critical size bone defect in the mandibular ramus of rats, using HA-collagen gel carriers (Lattanzi et al., 2008). In addition, Lin (Lin et al., 2013), found that periodontal ligament cells transduced with AdLMP-3 significantly increased mineralization *in vitro* by increasing Alkaline phosphatase (ALP), and bone sialoprotein gene expression. Moreover, Lattanzi (Lattanzi et al., 2013), reported the involvement of LMP in the molecular mechanisms acting during cranial suture morphogenesis, and underlying the premature fusion of calvarial sutures in human. In amniotic fluid stromal cells (AFSCs), Barba (Barba et al., 2012), showed that LMP-3 induced successful osteogenic differentiation of AFSC by inducing the expression of osteogenic markers and osteo-specific transcription factors.

In our study, we aim to find a new autologous regenerative therapy for bone regeneration by using direct reprogramming technique to

convert MEF cells into functional osteoblasts. For this purpose, we examined and evaluated the efficiency of using an osteo-inductive growth factor (hLMP-3) with different combinations of Yamanaka factors. We also tested the ability of this cocktail to induce bone formation in an orthotopic animal model.

2. Materials and methods

Procedures involving animals and their care conformed to the U.S. National Institute of Health guidelines (NIH Pub. No. 85-23, revised 1996). All animal experiments were reviewed and approved by the Institutional Animal Care and Use Committee of School of Animal Science and Technology, Yangzhou University. The procedures were performed in accordance with the Regulations of the Administration of Affairs Concerning Experimental Animals (China, 1988), and the Standards for the administration of experimental practices (Jiangsu, China, 2008). All the animals used in our study bought from the lab animal Centre, Jiangsu University, Zhenjiang, China.

2.1. Cells

2.1.1. Isolation and culture of MEF

Uterine horns from pregnant female mice (C57/BL) at 13 days post-coitum were removed, and embryos were harvested. After washing with PBS embryos were minced, incubated at 37 °C for 15 min in 0.25% trypsin EDTA (Gibco®, Grand Island, NY, USA) with gentle shaking. Trypsin was neutralized with an equal amount of MEF medium, and cells were collected by centrifugation (1000 rpm for 7 min). Afterwards, cells were re-suspended and cultured on gelatin coated dishes with MEF growth medium containing high glucose DMEM medium (11995-065, Gibco®) mixed with 10% FBS (HyClone), 4 mM L-glutamine (25030-081, Gibco®), and 1:100 penicillin-streptomycin at 37 °C with 5% CO₂. We examined the cells daily using an inverted microscope (Olympus TH4-200, Japan). Once confluent, cells were passaged 1:3 and the second passage cells were trypsinized and frozen at -80 °C. In our experiment, we used MEFs within three passages to avoid replicative senescence.

2.1.2. Induced pluripotent stem cells (iPSCs)

Murine iPSCs were previously reprogrammed in our lab Using mRNAs (El-Sayed et al., 2014).

2.2. Genetic materials

The codon-optimized hLMP-3 cDNA sequence obtained from (Pola et al., 2004), was synthesized, and cloned in T-Vector pMD19 (Takara, China) in Genscript company (Project ID. 7162905-1, China). The cDNA sequencing and primer design of hLMP-3 were also done in the same company (Genscript, China). Yamanaka factors (Oct 4 – Sox2 – c-Myc – Klf4) were amplified via polymerase chain reaction (PCR) from the mouse cDNA of the four pluripotency factors, previously cloned in our lab (El-Sayed et al., 2014). The primers' Sequences are listed in

Table 1
Primers used for amplification of the experiment genes.

Gene	Accession number	ORF primers
Oct-4	NM_013633	F: 5' CCCTCGAGGGCCACCTCCCCATGGCTGGACACC 3' R: 5' GCGTCGACGTTGGTGCCTCAGTTGAATGC 3'
Sox2	NM_011443	F: 5' CCCTCGAGGGATGATAACATGATGGAGACGGAGCT 3' R: 5' GCGTCGACGTTCACATGTGCGACAGGGCAGT 3'
c-Myc	NM_001177352	F: 5' CCCTCGAGGGATGCCCTCAACGTGAACCTTCACC 3' R: 5' GCGTCGACGTTATGCACAGAGTTCGAAGC 3'
Klf4	NM_010637	F: 5' CCCTCGAGGGATGAGGCAAGCCACCTGGGAGT 3' R: 5' GCGTCGACGCTACGTGGGATTTAAAAGTCCTC 3'
hLMP-3	AAK30569.1	F: 5' CCCTCGAGGGCTGGCCATGGATAGITTCAGAGGTGGTC 3' R: 5' GCGTCGACGTTCAGCCACTTGAGGCGGGCATCTG 3'

(Table 1). The primer used for Nanog expression (Accession number: AY278951.1) is F: 5'-GCAAGCGGTGGCAGAAAA-3' and R: 5'-TCCAGATGCGTTCACCAAGATAG -3'.

2.3. Lentiviral vectors

Construction of the virus expression vectors containing the transcription factors (4 Yamanaka factors and hLMP-3) were done in (Project ID. GM-Lc-01147, Genomeditech, Shanghai, China). Simply the cloned genes were sent to the company for cloning inside the lentivirus expression vector pGMLV-PE1 with GFP reporter. The amplified sequences were inserted into the multiple cloning site (MCS) of the expression vector, and verified by sequencing. Recombinant lentiviral particles were generated by co-transfecting lentiviral plasmids over-expressing genes of interest (pGMLVPE1- Oct4, pGMLVPE1- Sox2, pGMLVPE1- c-Myc, pGMLVPE1- Klf4 and pGMLVPE1- hLMP-3) together with the HIV packaging mix into 293 T lentiviral packaging cells and cultured in the 293 T cells for 48 h. Viral stocks were collected, concentrated by ultrafiltration, and titers were determined.

2.4. Fluorescence activated cell sorting (FACS)

We performed FACS analysis to assess the GFP expression in the transduced cells. Culture medium was removed, and the transduced cultured cells were washed twice with PBS. Afterwards, the cells were detached with trypsin (0.05%, Gibco®). Cells were collected, centrifuged and then re-suspended in PBS and kept on ice until the evaluation of GFP expression by a (FACSAria Flowcytometer) using FACSDiva software (Becton-Dickinson Immunocytometry Systems, BDIS, San Jose, CA).

2.5. In vitro osteogenic induction

The protocol used was modified after (Yamamoto et al., 2015), the preparation and dilution of the osteogenic medium components were done according to the protocol provided by the company. MEFs were re-suspended in a complete culture medium (CCM), and seeded onto 35-mm dishes (Corning®) (5×10^4 cells/dish) or a 24-well plate (Corning®) (1.2×10^4 cells/well) on day one. On the next day, the supernatant containing each lentivirus vector was mixed according to the different groups (MOI = 4), and supplemented with 4 μ g/mL polybrene (Genomeditech, Shanghai, China), then transferred to the fibroblast culture. Twenty-four hours later, the virus-containing medium was replaced with an osteogenic medium (OM) composed of a fresh complete culture medium supplemented with 50 μ g/mL ascorbic acid (Sigma Aldrich, China), 10 mM β -glycerol phosphate disodium salt (Sigma Aldrich, China), and 100 nM dexamethasone (Sigma Aldrich, China). The culture medium was changed every 2–3 days without trypsinization and reseeding all over the study period (21 days).

2.6. Quantitative real-time PCR (qRT-PCR)

Total RNA was extracted from the cell samples using TRIZOL® reagent (15596-026, Invitrogen) according to the manufacturer's protocol. After isolation, 1 μ g RNA was reverse-transcribed into cDNA using FastQuant RT Kits (With gDNase) (KR106, Tiangen, China). The cDNA samples were analyzed by qRT-PCR in a 7500 Real-Time PCR system (Applied Bio systems) using Super Real Premix plus (SYBER-GREEN) (FP205, Tiangen, China). The conditions for qRT-PCR were as follows: 95 °C for 15 min.; followed by 40 amplification cycles (95 °C for 10 s.; 60 °C for 32 s.). Sequences of the qRT-PCR primers are listed in (Table 2). The primers were designed and manufactured at (Takara, China). Relative quantification was calculated with $2^{-\Delta\Delta Ct}$ and normalized to β -actin. Data were presented as levels related to the expression level in control cells.

Table 2

Primers used for the qRT-PCR.

Gene	forward primer 5'....3'	reverse primer 5'....3'
β -actin	CATCCGTAAGACCTCTATGCCAAC	ATGGAGCCACCGATCCACA
Runx2	TGCAAGCAGTATTACACAGAGG	GGCTCACGTCGCTCATCTT
Osx	GCGACCACTTGAGCAAACATC	CGGCTGATTGGCTTCTTCTT
BMP-2	TGATGTGGGTGGAATGACT	CAGCAAGGGAAAAGGACAC

2.7. In vitro mineralization assay

Early osteogenic differentiation was evaluated by ALP staining. The matrix mineralization was evaluated by ALZ staining, and VK staining. The staining intensity was quantified using the Fiji is just Image J (National Institutes of Health, Bethesda, MD, USA) (Schindelin et al., 2012).

2.7.1. Alkaline phosphatase (ALP) staining

Histochemical staining was performed with a BCIP/NBT alkaline phosphatase color development Kits (C3206, Beyotime, China) according to the manufacturer's protocol. The cells were washed with PBS buffer, then fixed with 4% formalin at room temperature for 2 min. The cells were then washed 3 times with PBS. After the last washing, an appropriate amount of BCIP/NBT staining solution was added to ensure that the sample is fully covered. After the addition of the working solution, cells were incubated in the dark at 37 °C for 5–30 min. until the desired color developed. The BCIP/NBT stain working solution was removed, and cells washed with distilled water for 1–2 times to stop the color reaction.

2.7.2. Alizarin Red (ALZ) staining

The cells were washed with 1 × PBS, and fixed in 10% formaldehyde in 1 × PBS for 15 min. After fixation the cells washed with distilled water for 2–3 times. Cells incubated in 40 mM Alizarin red staining solution for 5 min. at the dark. Finally, cells washed by distilled water 4 times to remove the excess staining. The alizarin red staining solution was prepared by diluting the alizarin red staining powder (A5533, Sigma-Aldrich) in distilled water.

2.7.3. Von Kossa (VK) staining

For staining by the von Kossa method, the cells were washed with PBS, fixed with 10% formalin and stained with freshly prepared 5% silver nitrate solution for 30 min. with exposure to UV light. After washing with distilled water 3 times, the cells were treated with 5% sodium thiosulfate solution for 3 min. to remove any remaining silver nitrate. Final washing with distilled water repeated for 3 times. The silver nitrate solution (5%) prepared by diluting the silver nitrate powder (GB12595-90 Beijing HenGye Zhongyuan co., China) in distilled water. The same diluent used for preparation of the sodium thiosulfate (217263, Sigma-Aldrich).

2.8. Immuno-fluorescence

The cells were rinsed briefly with PBS, and fixed for 20 min. with 4% paraformaldehyde in 0.1 M phosphate buffer (pH 7.4) at room temperature. The cells were permeabilized for 10 min. with 0.1% Triton X-100 in PBS, to allow the entrance of the specific antibodies into the cells, and then blocked for 45–60 min with 4% bovine serum albumin in PBS at room temperature. Cells were incubated overnight (~ 16–18 h) at 4 °C with anti-OCN (1: 500; sc-376726, Santa Cruz). The cells were then washed 3 times with the washing buffer. This was followed by incubation with the following secondary antibody: Alexa Fluor 647-labeled anti-mouse IgG (1:500; ab150115, Abcam). Following a final round of 3 washes with the wash buffer, nuclei were counterstained using DAPI (1 mg/mL PBS; Invitrogen, Carlsbad, CA,

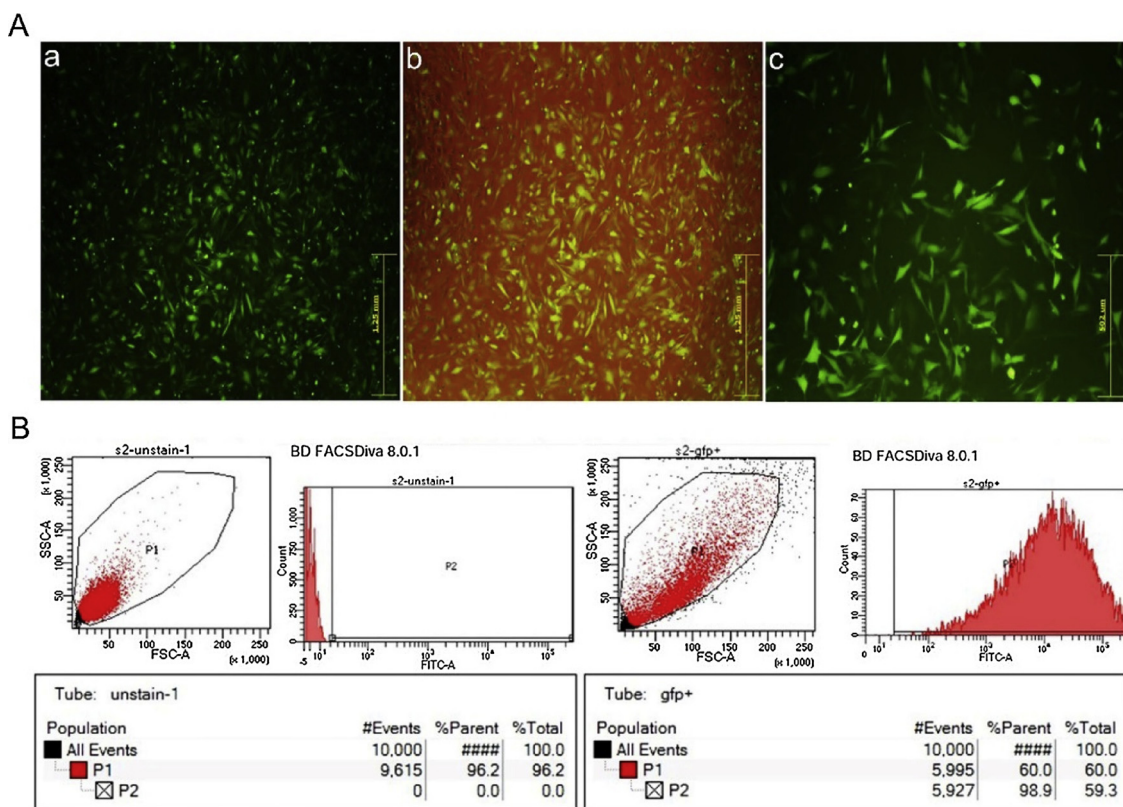


Fig. 1. Transduction of MEF cells with pGMLVPE1-EGFP. (A) The fibroblast cells were transduced with pGMLVPE1-EGFP vector. a) Showed MEF expressed GFP b) Intermediate phase; while c) The green fluorescent phase of the transduced cells (higher magnification); (B) FACS analysis of the transduced MEF cells with pGMLVPE1-EGFP with normal non-transduced MEF used as negative control (GFP = 0%); while MEF transduced with pGMLVPE1-EGFP 48 h. Post-transduction (GFP = 98.9%). (For interpretation of the references to colour in this figure legend, the reader is referred to the web version of this article.)

USA). For immune staining of Nanog, Oct4, and c-Myc the following conjugated antibodies were used: anti-Oct4 (Alexa Fluor® 647) (ab196585, Abcam), anti-c-Myc antibody (Alexa Fluor® 647) (ab190560, Abcam), and anti Nanog (Alexa Fluor® 647) (NB100-58842AF647, Novus Biologicals).

2.9. Western blot analysis

All steps were done according to the manufacturer's protocol, using a Bio-Rad system (Bio-Rad, USA). The cell lysates were collected by RIPA buffer (P0013B, Beyotime, China) supplemented with phenyl methane sulfonyl fluoride (Beyotime, China). Following centrifugation at 12,000 g at 4 °C for 10 min., the supernatant was collected and the protein concentration was determined using a BCA protein assay kit (Beyotime, China). Protein samples were heated for 10 min. at 95 °C, and then separated by 10% sodium dodecyl sulfate polyacrylamide gel electrophoresis (SDS-PAGE) (20 µg protein/lane). Afterwards, blotted onto poly vinylidene fluoride (PVDF) membranes (Solarbio, China) using Trans-Blot SD system (Bio-Rad). The membranes with target proteins were blocked with BSA blocking buffer (CW2143S, CWBIO, China) at room temperature for 2 h., and then incubated with the primary antibody OCN (1: 500; sc-376726, Santa Cruz) at 4 °C overnight. After washing for three times, the corresponding secondary antibody HRP labeled goat anti mice IgG (1: 2000; 665739, Merck Millipore) was added. The membranes were incubated at 37 °C for 2 h. Followed by washing using TBST (CW0043S, CWBIO, China). Bands were visualized by enhanced chemiluminescence method (cECL) western blot kits (CW0048 M, CWBIO, China) using FluorChem Q system (Protein simple, USA). β-actin (AA128, Beyotime, China) was used as a loading control. The protein band intensity was quantified using the Fiji is just Image J program (National Institutes of Health, Bethesda, MD, USA).

2.10. Surgical procedure and cell transplantation

We used 12 apparently healthy adult male Sprague Dawley (SD) rats. Their body weight ranged from 250 to 300 g m. The age of the rats was approximately 8 weeks old. Rats were anesthetized with an intramuscular injection of a standard anesthetic cocktail consisting of ketamine hydrochloride (50 mg/kg) (Gutian, China), and xylazine (6 mg/kg) (Yansuan sailaqin zhushey, China) (Hall et al., 2001). A unilateral cortical bone defect ~8 × 3 mm was created at the diaphysis of the right femur of SD rat. This defect was filled with Matrigel high protein concentration (Corning®) with or without COL transduced cells. Cells were re-suspended in a mixture of medium and Matrigel (the final cell concentration ~10⁶ cells/mL). The left femur considered as a positive control without any surgical intervention.

2.11. Radiographic and histological examination

To examine and monitor the progression of bone healing, serial radiographs of the operated femurs were taken every 4 weeks. Briefly, animals were placed onto their back on an approximately 3 cm elevated stage and their operated leg taped down with their right thigh in full extension to help get a clear unobstructed view of the bone defect. Digital X-rays (Varian medical system) were taken at the Animal Hospital in Yangzhou University (voltage of 64 kV and a current of 2 mAs). Specimens for histological examination were then fixed in 10% buffered formalin for 48 h. Femora were decalcified in 10% EDTA at room temperature for (45–60 days) (Wang et al., 2017b). Decalcified bone specimens were stained with hematoxylin and eosin (H&E) to assess the bone formation in the defect area. Frozen sections were performed by immediate fixation of the specimens in 4% PFA, followed by decalcification step. They were sectioned on a cryostat (LEICA

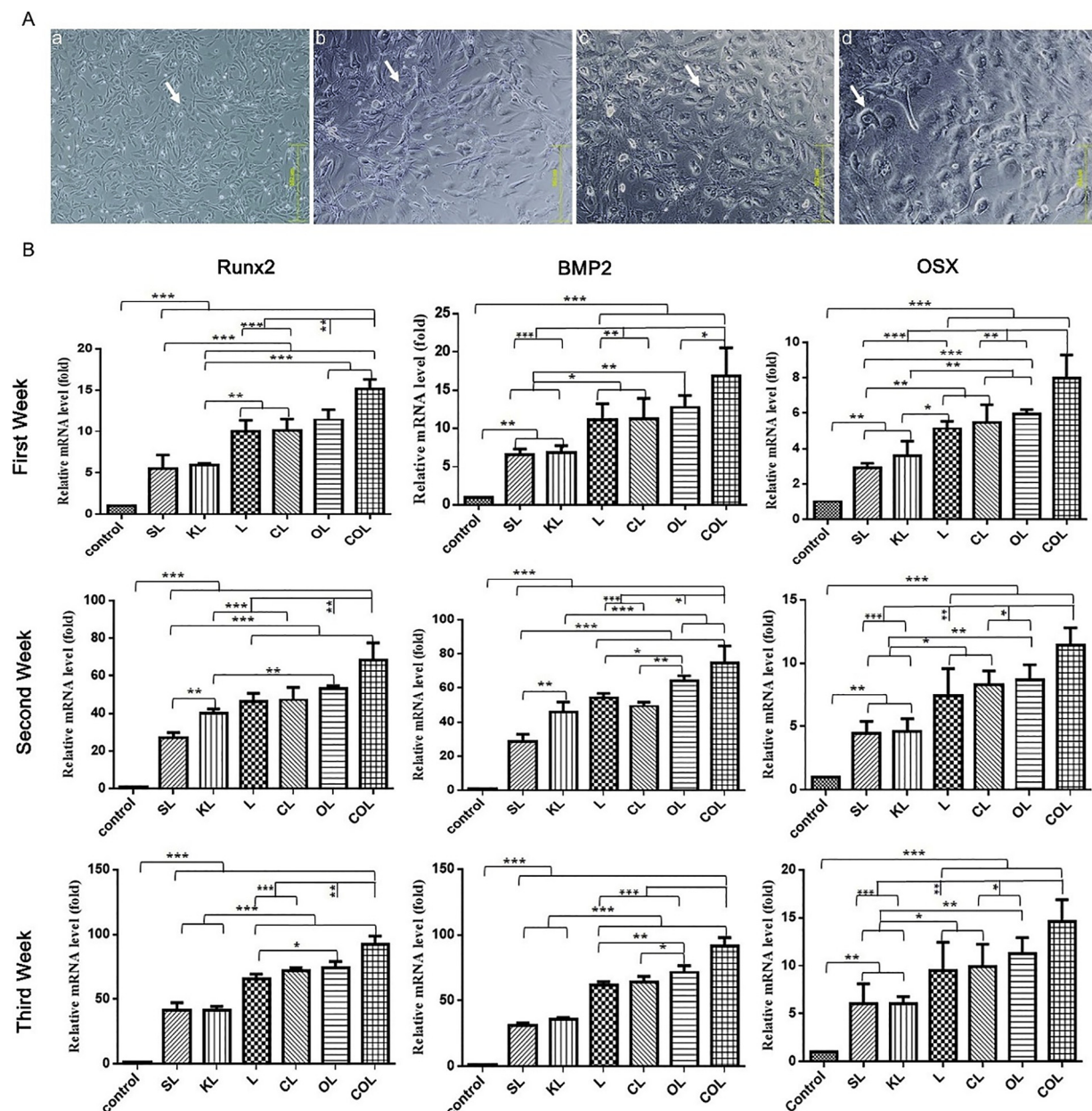


Fig. 2. Morphological and molecular changes during conversion of MEF to osteoblast cells. (A) Phenotypic changes during conversion process in the COL group a) showed the characteristic spindle shape appearance of fibroblast, b) the cell shape changed to a flat appearance; while c) revealed the relative polygonal shape, and finally d) after 21 days post transduction showed the classical cuboidal appearance of osteoblast (white arrows); (B) Expression level changes in bone specific markers using qRT-PCR analysis of Runx2, BMP-2, and OSX. All quantitative data were expressed as the means \pm standard deviation ($n = 3$). P was calculated at 3 levels (*: $P < 0.05$), (**: $P < 0.01$), and (***: $P < 0.001$). hLMP-3 group (L), Oct4 + hLMP-3 (OL), Klf4 + hLMP-3 (KL), Sox2 + hLMP-3 (SL), c-Myc + hLMP-3 (CL), and c-Myc + Oct4 + hLMP-3 (COL).

CM1950), after embedding in Tissue-Tek O.C.T. compound (SAKURA, USA), and frozen in liquid nitrogen at 18 μ m serial sections coronally. Tissue sections obtained from rats treated with Matrigel seeded with GFP-positive cells were analyzed using fluorescence microscopy (Olympus TH4-200, Japan), in order to detect the persistence of GFP-positive cells after transplantation. In addition, immune staining with anti-OCN (sc-376726, Santa Cruz) was performed, and visualized with Alexa Fluor 647-labeled anti-mouse IgG (ab150115, Abcam).

2.12. Statistical analysis

All quantitative data were expressed as the means \pm standard deviation ($n = 3$). Statistical analyses were performed using SPSS® software V.21 (Chicago, IL). Statistical significance was determined using

one-way analysis of variance (ANOVA) followed by a post hoc test (multi-group comparison). P was calculated at 3 levels ($P < 0.05$), ($P < 0.01$), and ($P < 0.001$). GraphPad Prism software V.6 used for statistical illustrations (GraphPad Software, La Jolla, CA, USA).

3. Results

3.1. Lentivirus transduction efficiency and the multiplicity of infection

Sub-confluent MEFs at P3 were infected with the GFP lentivirus vector to determine the correct amount of lentivirus particles to be used for reprogramming. Cells transduced with varying amounts (2, 4, 6, 8, 10, 15, 20, 25, and 30 MOI) of lentivirus GFP reporter with different concentration of polybrene (0, 2, 4, 6, and 8 ng/ μ L). After 48 h, cells

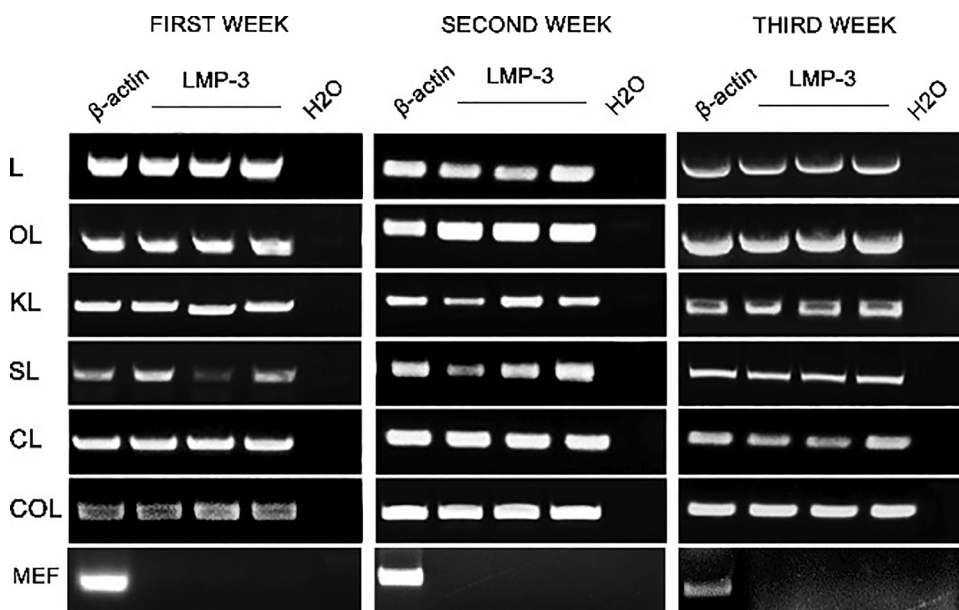


Fig. 3. Molecular characterization of the hLMP-3 in the transduced MEF. Total RNA was isolated from cells in different groups, and were used for RT-PCR to detect the expression of hLMP-3. Our results were normalized to β -actin as an internal control. hLMP-3 group (L), Oct4 + hLMP-3 (OL), Klf4 + hLMP-3 (KL), Sox2 + hLMP-3 (SL), c-Myc + hLMP-3 (CL), and c-Myc + Oct4 + hLMP-3 (COL).

were examined using the fluorescent microscope to detect the cell conditions and the GFP expression (Fig. 1A). We found that the best result obtained was MOI = 4 and polybrene concentration = 4 ng/ μ L. The FACS analysis showed that the percentage of GFP positive cells in the transduced cells at MOI 4 with the polybrene concentration of 4 ng/ μ L reached 98.9%, when compared with the non-transduced MEF (Fig. 1B).

3.2. Induction of osteoblasts from MEF by the combination of hLMP-3 and Yamanaka factors

We assessed the ability of different combinations of the 4 reprogramming factors (Oct4, Sox2, c-Myc, and Klf4) with an osteogenic factor (hLMP-3) to induce functional osteoblasts from MEF. Lentivirus vector encoding hLMP-3 and the Yamanaka factors were transduced into MEF as following: hLMP-3 alone (L), hLMP-3 + Sox2 (SL), hLMP-3 + Klf4 (KL), hLMP-3 + c-Myc (CL), and hLMP-3 + Oct4 (OL). After transduction, cells were cultured in an osteogenic medium. Assessment of osteoblast like characteristics, and analysis of mRNA expression of bone specific markers BMP2, Runx2, and Osterix (OSX) were performed.

After transduction, we observed morphological changes in the transduced cells with hLMP-3 alone or with different Yamanaka factors combinations from the elongated spindle shape appearance of fibroblasts in the control group. After culturing in an osteogenic medium, the spindle-shaped cells switched to retracting flat ones, followed by relatively polygonal shape. Cells in the control group showed a relatively greater cell number than the other groups on day 7. After 14 days, cells induced to osteoblast formation displayed clusters with high cell density and large amounts of an ECM as detected by mineralization assay; while untreated control cells maintained their phenotypes. Meanwhile, more cells in the treatment groups showed the characteristic appearance of osteoblastic cells (classical cuboidal shape) (Fig. 2A).

Quantitative real time PCR (qRT-PCR) analysis showed elevated expression of osteogenic markers in both CL and OL groups in comparison with hLMP-3 alone group. On the other hand, both SL and KL groups downregulated the osteogenic potency of hLMP-3. These results indicated that both Oct-4 and c-Myc may contribute in the induction process of the osteoblast-like cells beside the osteogenic factor hLMP-3. On contrary, both Sox2 and Klf4 didn't play the same role, but they declined the expression of the osteogenic markers, when combined with

the hLMP-3. Based on these findings, we combined both c-Myc and Oct-4 with hLMP-3 in another group (COL) to find out if any synergistic effect of this combination is existed. Surprisingly, we found a remarkable elevation was elicited by combining both c-Myc and Oct-4 with hLMP-3 (Fig. 2B).

3.3. Molecular characterization of hLMP-3 in the transduced cells

In addition to the GFP expression in the transduced cells, we further confirmed the hLMP-3 gene expression in the reprogrammed cells by detecting its mRNA level. The expression of the hLMP-3 gene is a key factor in our experiment because it's the osteogenic factor used to induce osteoblast cells. The results demonstrated that robust expression of the hLMP-3 was observed all over the experiment time in comparison to the negative expression of the hLMP-3 in the MEF cells in the control group (Fig. 3).

3.4. Conversion efficiency of induced osteoblasts from c-Myc, Oct-4 and hLMP-3 combination

Based on the results of qRT-PCR, we further characterized the generated osteoblast cells using the *in vitro* mineralization assay to compare the hLMP-3 group and the cocktail (c-Myc, Oct-4, and hLMP-3) group with the control cells. The mineralization assay was performed every week after transduction for three consecutive weeks. The *in vitro* mineralization assay includes: ALP, ALZ and VK staining. The L group induced significant ALP expression detected 7 days post transduction, but more intensive ALP expression was observed in the COL group. Both ALZ and VK staining were negative in all groups on day 7 as they were considered as late markers for osteogenesis. After 14 days post transduction, ALZ staining showed that the mineralized matrix began to appear in culture, as a sign of osteogenic differentiation in both L and COL groups. VK staining didn't reveal clear results at this time point. Finally, on the 21st day post transduction, ALZ and VK staining showed calcium deposition and bone nodules formation. The results from the matrix mineralization assay were consistent with that of qRT-PCR. Our findings demonstrated that using (c-Myc and Oct4) with hLMP-3 promoted the conversion of fibroblasts to osteoblasts, as detected by increased calcified bone matrix generation capacity (Fig. 4A).

Another crucial marker of late osteogenic differentiation was determined by detection of OCN protein production using both immunofluorescent staining and western blot analysis. The combination of

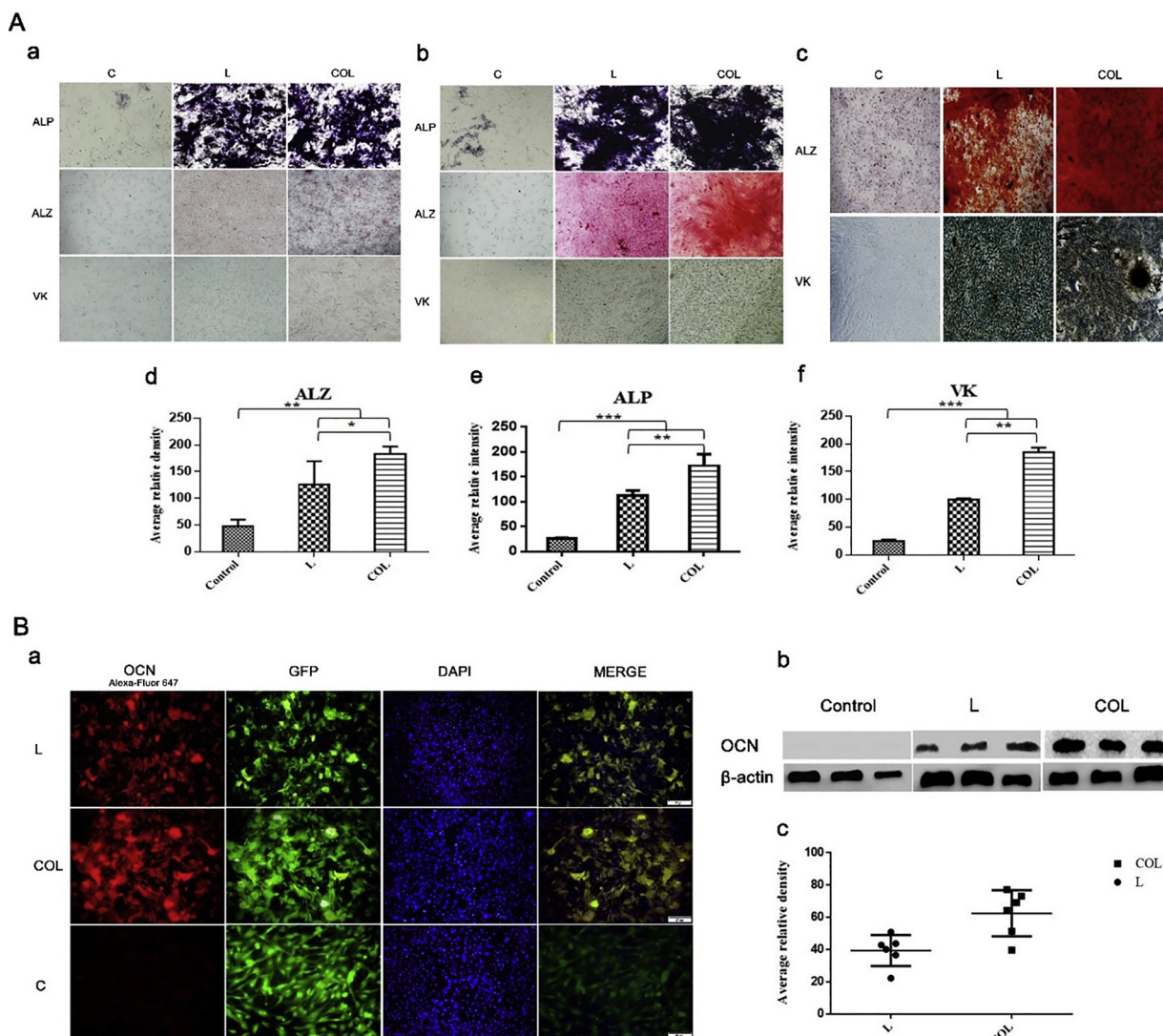


Fig. 4. Characterization of the induced osteoblasts from c-Myc, Oct-4 and hLMP-3 combination. (A) *In vitro* mineralization assay of L & COL groups. a) After 7 days post transduction, the expression of the ALP was detected in both L and COL groups, b) ALZ staining used to evaluate the level of mineralized nodule formation. Mineralized nodule formation started at 14 days post transduction in both L & COL groups, c) After 21 days post transduction, positive staining of VK revealed complete osteogenic differentiation of the MEF to osteoblast like cells. The magnification of (a, b and c) is 40X; while d, e, and f are the staining intensity of ALP, ALZ, and VK respectively. Quantification of the staining intensity performed with Fiji is just Image J software. P was calculated at 3 levels (*: $P < 0.05$), (**: $P < 0.01$), and (****: $P < 0.001$); (B) Osteocalcin expression in the generated osteoblast cells. a) The transduced cells were immune-stained with a specialized marker of late osteoblast differentiation (OCN) after 21 days post transduction. b) The expression of OCN on protein level using western blot analysis. The mean of average relative density of the WB bands were measured using Fiji is just Image J software. The mean and SD were plotted using Graphpad prism version 6. hLMP-3 group (L), Control group (C), and c-Myc + Oct4 + LMP-3 (COL).

c-Myc, Oct4 and hLMP-3 induced stronger OCN expression than hLMP-3 alone (Fig. 4B). Thus, it was considered that the combination of COL has the strongest capability of inducing osteoblast-like cells among our study groups. Meanwhile, we can conclude that combining of pluripotency factors (c-Myc – Oct4) with lineage specific factor (hLMP-3) which termed as direct reprogramming is superior than using lineage specific factor alone (Transdifferentiation).

3.5. MEF were directly reprogrammed into osteoblast like cells without passing through an intermediate pluripotent Stage

MEF transduced with c-Myc, Oct4, and hLMP-3 were immune-stained with anti-Nanog antibody every 5 days from the first day post transduction till the 15th day. Cells were thoroughly examined under fluorescent microscopy every time point. Nanog expression as an indispensable transcription factor for pluripotency was not significant during the entire experimental period (Fig. 5A). For further

confirmation, we performed RT-PCR analysis to detect the Nanog expression, and the same negative result was obtained (Fig. 5B). These results demonstrated that, during the conversion process, no intermediate pluripotent stage was present.

Moreover, we immune-stained the transduced MEF cells with anti-Oct4 and anti c-Myc one day after transduction to detect their expression level, and also after 15 days post transduction in comparison with the iPSCs as a positive control (Fig. 6). We found a significant decrease in their expression level in comparison with iPSCs with only small subset showed levels of fluorescence scarcely above background.

3.6. Osteoblasts from c-Myc, Oct-4 and hLMP-3 combination induced bone repair after transplantation into a unilateral cortical bone defect in rat

To examine whether the generated osteoblast can enhance bone formation, we transplanted the generated osteoblast like cells from the COL group into a unilateral bone defect created surgically at the right

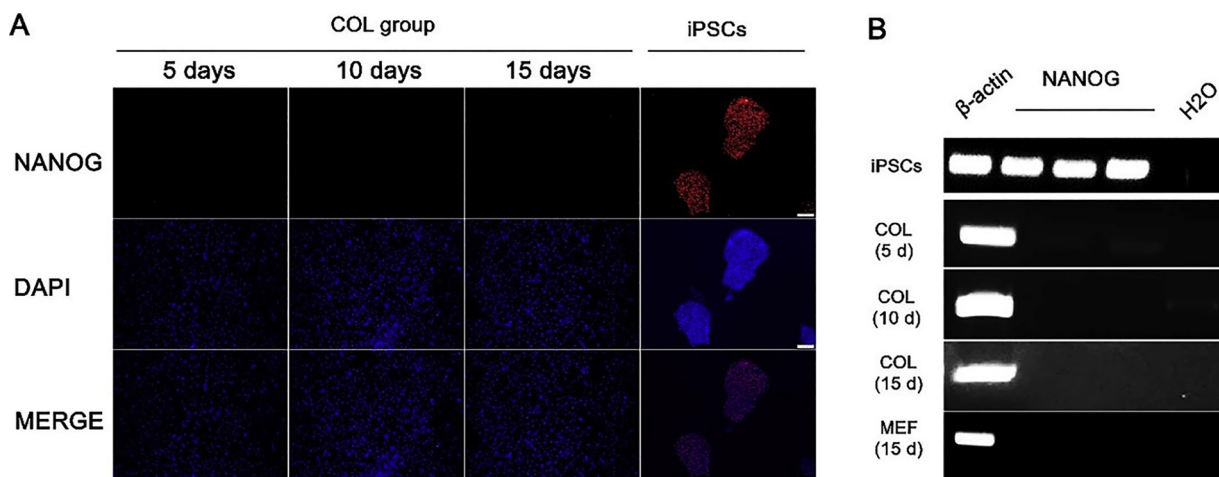


Fig. 5. Molecular characterization of Nanog in the reprogrammed MEF. A) MEF were transduced with c-Myc, Oct4, and hLMP-3 and stained with anti-Nanog antibody and DAPI on the indicated days. No Nanog-positive cells were observed. As a positive control, murine iPSCs were strongly stained with anti-Nanog antibody; (B) Total RNA was isolated from cells in different groups, and were used for RT-PCR to detect the expression of Nanog. iPSCs were used as a positive control. Our results were normalized to β -actin as an internal control. c-Myc + Oct4 + hLMP-3 (COL).

femurs of SD rats (Fig. 7). Bone repair was assessed at 30 d and 60 d post transplantation by macroscopic, radiographic, and histological examinations. Macroscopically, the healing process showed that the induced defect parts were totally regenerated in the COL group; whereas bone defects remained in the control group in which Matrigel was used without cell implantation (Table 3). Radiographically, the induced defect in COL group was covered with callus formation; while control group didn't show the same signs. Furthermore, the induced defect area showed more radiopacity in COL group than the control ones (Fig. 8A). Histological examination also revealed a bridging callus formation at the defect area in the COL group with presence of GFP positive cells as a sign of transgene persisted expression of the transplanted cells *in vivo* over time after the implantation in fresh tissue sections. The transplanted cells also showed a remarkable OCN expression after immunostaining in comparison with the control group (Fig. 8B). These results proved that the transplanted cells retained the osteoblast-like characteristics and were able to produce the bone matrix *in vivo*.

4. Discussion

In the present study, we reported for the first time the effect of combination of Yamanaka factors with hLMP-3 to induce osteoblast cells from MEF. The generated cells characterized by the classical cuboidal appearance of the osteoblast cells, and produced a mineralized bone matrix. Our results revealed that co-transduction of c-Myc and Oct4 with hLMP-3 increased the hLMP-3 osteogenic potency. In contrast, Sox2 and Klf4 downregulated the osteogenic potency of the hLMP-3. We didn't detect any intermediate pluripotency stage during reprogramming by using Nanog as a marker for pluripotency. In addition, the generated osteoblasts facilitated bone repair in unilateral femoral bone defect in SD rat after transplantation.

In this study, the hLMP-3 gene has been used to induce osteoblast formation, for its remarkable advantages. LMP-3, in contrast to the BMPs, is a non-secreted protein; thereby reduce any possible drawbacks caused by the high expression levels of an exogenous osteogenic mediator. In addition, several studies reported that hLMP-3 osteoinductive potency is partially mediated through being upstream of the main osteogenic pathways inside the cell, such as upregulation of the BMP-2 gene (Minamide et al., 2003; Pola et al., 2004; Yoon et al., 2004). We also found that lentivirus transduction of hLMP-3 induced matrix mineralization as detected by the early osteogenic marker ALP, and late markers as positive ALZ& VK staining. Our results showed upregulation

in the early osteogenic marker expression Runx2, and late osteogenic marker OCN. This up regulation in Runx2 expression was due to hLMP-3 stimulation, as it is stated that signals in the upstream of key transcription factors are essential for neogenesis (Lin et al., 2013). Other reports (Minamide et al., 2003; Pola et al., 2004; Yoon et al., 2004) revealed that LMP induced the expression of BMPs, Runx2, Osterix, BSP, OCN, OPN and ALP. On the other hand, Lin (Lin, 2010), reported non-significant expression of Runx2 and OCN, after AdLMP-3 over-expression because the possible toxic effect of adenovirus used. Moreover, hLMP-3 could induce the osterix promoter, and the expression of chromatin remodeling complexes in adult MSC, which have been reported to stimulate the BMP-2 related pathway (Young et al., 2005). Lattanzi (Lattanzi et al., 2008), revealed that hLMP3 stimulated certain osteogenic factors that induce osteogenesis in both undifferentiated and differentiated cell types. LMP3-engineered cells have the great advantage to release these osteogenic factors at physiologic levels *in situ*.

Direct lineage reprogramming has been performed successfully in generating many tissue-specific cell types and also their stem-like precursors, such as: neurons, neural stem cells, cardiomyocytes, chondrocytes, hepatocytes, hepatic stem cells, and blood progenitor cells (Efe et al., 2011; Hiramatsu et al., 2011; Huang et al., 2011; Ieda et al., 2010; Outani et al., 2013; Pang et al., 2011; Qian et al., 2012; Szabo et al., 2010; Thier et al., 2012; Vierbuchen et al., 2010; Yu et al., 2013). Previous studies demonstrated direct reprogramming in the orthopedic field were also conducted (Wang et al., 2017a; Yamamoto et al., 2015). Most of their results were consistent with our results in many points, especially the confirmation that during the reprogramming process, no pluripotency was detected, which is a very important point to avoid post transplantation tumors and teratomas.

Our results showed a remarkable effect of combining Oct4, c-Myc, with hLMP-3 during reprogramming of MEF to osteoblast cells. In agreement with Yamamoto (Yamamoto et al., 2015), who successfully converted fibroblasts directly into osteoblasts by transducing some transcription factors (Runx2, Osterix, Oct4, and *t*-Myc). They found that among the four Yamanaka factors, only Oct4 may play an important role; while the other factors might not have the same importance for producing the bone matrix.

Oct4 plays a vital roles in maintaining pluripotency and reprogramming of iPSCs (Takahashi et al., 2007; Takahashi and Yamanaka, 2006; Yamanaka, 2007). Shu (Shu et al., 2013), recently reported that Oct4 and Sox2 are meso-endodermal and ectodermal differentiation cues, respectively, and that the balance between these counteracting signals may help during reprogramming process. In the present study,

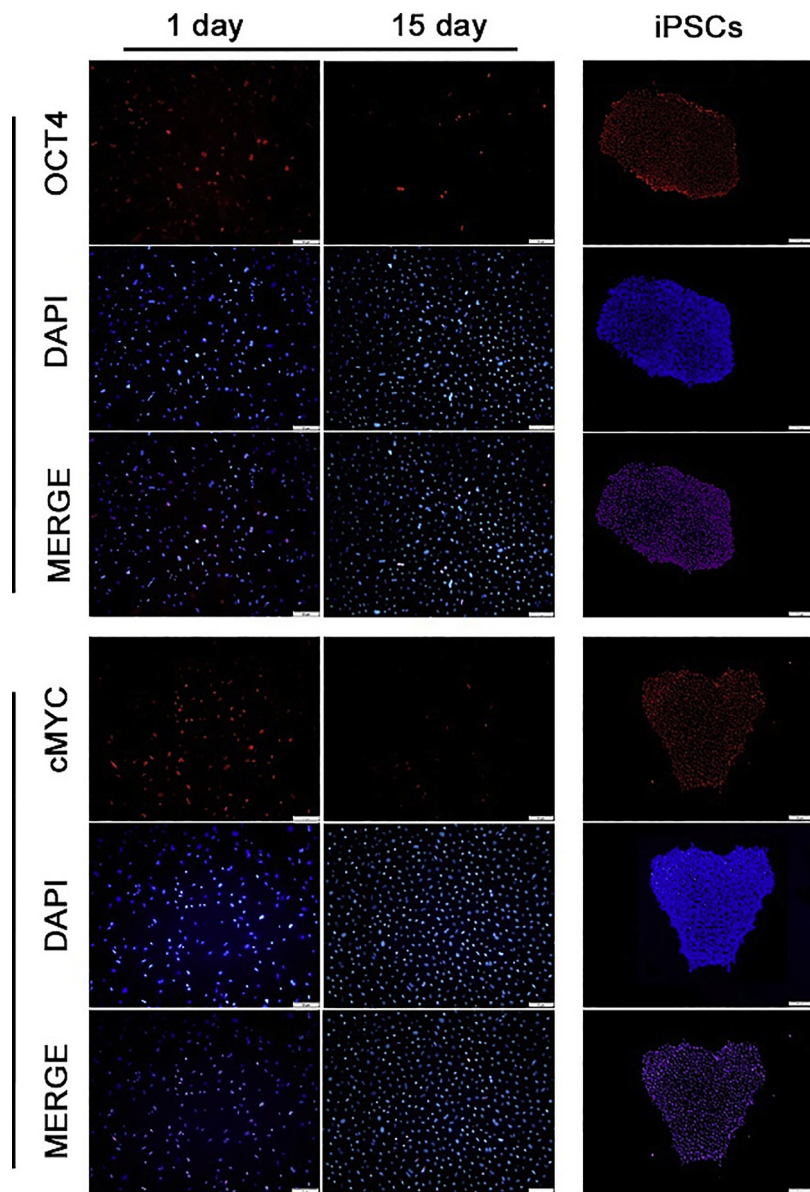


Fig. 6. Molecular characterization of Oct4 and c-Myc in the reprogrammed MEF. A) MEF were transduced with c-Myc, Oct4, and hLMP-3 and stained with anti-oct4, anti- c-Myc antibodies and DAPI on the indicated days. A sharp decline was observed in both Oct-4 and c-Myc expression from the 1st day post transduction till the 15th day. As a positive control, murine iPSCs were strongly stained with anti-Oct4 and anti- c-Myc antibodies.

we found that Oct4 is an important factor for the direct reprogramming technique, based on the elevated expression of the osteogenic markers in both OL and COL groups. Several researches agreed with our findings (Mizoshiri et al., 2015; Yamamoto et al., 2015), they found that Oct4 is essential for the direct reprogramming of osteoblast like cells. Therefore, they suggested that Oct family members play their role during direct reprogramming to osteoblasts by regulating the transcription of downstream gene groups, which is different mechanism from the iPSCs induction (Mizoshiri et al., 2015).

The proto-oncogene c-Myc is another Yamanaka factor (Nakagawa et al., 2008). Myc is related to cell proliferation, cell growth factors, differentiation and apoptosis. In our findings, c-Myc with hLMP-3 or in combination with Oct4, and hLMP-3 showed efficient osteoblast induction. Other reports demonstrated the importance of Myc in different direct reprogramming techniques of fibroblast into neural cells (Han et al., 2012; Thier et al., 2012), chondrocyte (Hiramatsu et al., 2011), and osteoblast (Yamamoto et al., 2015). The transduction of Oct4 and L-Myc induced osteoblast-like phenotypes in fibroblasts, these cells moderately expressed endogenous Runx2, but these cells are less

similar to osteoblast cells (Mizoshiri et al., 2015). In the same context, Li (Li et al., 2017), proposed another reprogramming module that effectively produced osteoblast cells via reprogramming of fibroblast cells using a single transcriptional factor Runx2 with small molecules replaced the effect of Oct4 and Myc (CHIR and forskolin). In a different pathway, Mizoshiri (Mizoshiri et al., 2015), introduced either Oct3/4, Oct6 or Oct9 and one of the Myc family members together in fibroblast to induce an osteoblast-like phenotype. However, in their work, c-Myc showed the highest induction effect on osteoblast-like phenotype followed by L-Myc and N-Myc, respectively.

We observed in our study that overexpression of Sox2 with hLMP-3 decreased the osteogenic potency of LMP-3, in contrast to Oct4 and c-Myc. In the field of differentiation decisions, there are contradictory results about the role of Sox2. Sox2 plays an essential role in the maintenance of undifferentiated lineage progenitors (Ellis et al., 2004; Pevny and Nicolis, 2010), and it's a critical reprogramming factor for the conversion of somatic cells to (iPSCs) (Takahashi and Yamanaka, 2006). It has been reported that Sox2 inhibited the osteogenic differentiation; whereas it is required for efficient adipogenic differentiation

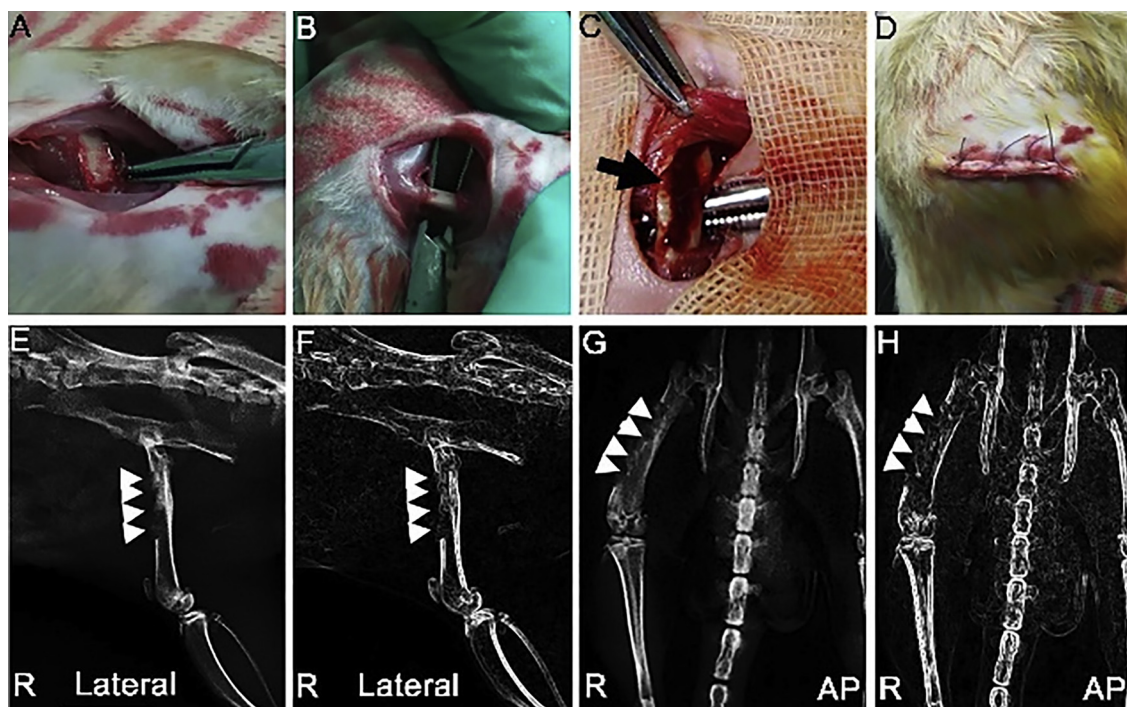


Fig. 7. Unilateral cortical bone defect in the right femur of SD rat. (A) Skin incision was done in the right thigh and the muscles exposed. (B) Showed the femur after complete dissection from the surrounding muscle and fascia (white arrow). (C) The cortical bone defect was created in the femur (D) suturing of the wound after operation (E&G) X-ray films (lateral and AP positions) taken directly after operation to detect the defect and complications if existed. The defect appeared as a radiolucent area (white arrows). (F&H) the same pictures processed with Image J software to clarify the extent of defect.

Table 3
Summary of the *in vivo* experiment results.

Time point	Induced femoral defect		Number of positive rats		Number of negative rats	
			COL	Matrigel	COL	Matrigel
	COL	Matrigel	COL	Matrigel	COL	Matrigel
4 weeks	3	3	3	0	0	3
8 weeks	3	3	3	0	0	3

of MSC via Dkk1 upregulation and Wnt signaling inhibition (Park et al., 2012). Schonitzer and his colleagues (Schönitzer et al., 2014) observed that ectopic expression of Sox2 kept the MSC in an undifferentiated state and concomitantly, decreased their osteogenic and adipogenic differentiation potential. However, in the osteoblast lineage, Sox2 is expressed at relatively low levels in immature cells, both *in vitro* and *in vivo* (Mansukhani et al., 2005). Over expression of Sox2 can increase sphere formation, and hinder osteoblast differentiation. Sox2 also plays an inhibitory role on FGF on the pro differentiation Wnt pathway by binding to β -catenin; a major effector of canonical Wnt signaling, and inhibiting its transcriptional effect (Ambrosetti et al., 2008; Mansukhani et al., 2005). Ding (Ding et al., 2012), found that overexpression of Sox2 increased the proliferation of C3H10T1/2 cells, activation of Wnt/ β -catenin, and p38MAPK pathways. On contrary, when they cultured the cells in an osteogenic differentiation medium, they found an inhibition of both ALP and mineralized nodules formation with a remarkable decrease in the osteogenic genes' expression. Besides, an inhibition in both Wnt/ β -catenin and p38MAPK pathways.

Based on our qRT-PCR results, we found that Klf4 overexpression attenuated the osteogenic induction of hLMP-3 in MEF cells. Although Klf4 plays a crucial role in various biological processes such as proliferation, differentiation, survival, and development (Evans and Liu, 2008). Michikami (Michikami et al., 2012), reported that Klf4 inhibited osteoblast differentiation. Their findings revealed that after Klf4 over-

expression in the osteoblast cells *in vivo*, the formation of calvarial bones was severely impeded. In the same context, Kim (Kim et al., 2014), found that Klf4 physically associated with Runx2 to inhibit the DNA binding and its transcriptional activity. Repression of Runx2 transcriptional activity by Klf4 resulted in both decrease in ALP and BSP expression, and inhibition of osteoblast differentiation and function. Barba (Barba et al., 2012), discovered that LMP-3 induced the osteogenic differentiation of AFSCs by inactivation of Klf genes, and further upregulation of osteo-specific transcription factors. All the previous reports together with our findings collectively support that Klf4 is a potent negative regulator of osteoblast differentiation and function *in vitro*.

The transplantation of MSCs has been performed over years to treat bone loss in many surgical situations (Liu et al., 2014). This transplantation procedure aid in bone repair, by involvement of osteoblasts originated from the graft in bone regeneration. Autologous MSC transplantations faces some road blocks during clinical application. However, especially in elderly patients, age-related decrease the potential of stem cell for differentiation into osteoblasts (Kim et al., 2012). Such problems may be eliminated by using the direct reprogramming strategy, which has the advantage of generating osteoblasts in large numbers from fibroblasts isolated from patients by a less-invasive intervention (Huschtscha et al., 2012). Fibroblasts are characterized by high proliferative capacity, which does not reduce with age (Cristofalo et al., 1998; Huschtscha et al., 2012). Thus, direct reprogramming may be performed as another solution for patients in whom transplantation of MSC is not the ideal therapy.

Our *in vivo* work demonstrated the effective treatment regarding the healing time and efficiency of an induced bone defect in an orthotopic rat model using MEF reprogrammed with cocktail of transcription factors (c-Myc and Oct4) with hLMP-3. The use of pre-differentiated osteoblasts has been shown to enhance the rate and extent of bone regeneration (Jayakumar and Di Silvio, 2010). Osteoblasts synthesize bone-specific proteins and enzymes, including ALP, OCN, and type I collagen. Our findings must be built on to improve this kind of

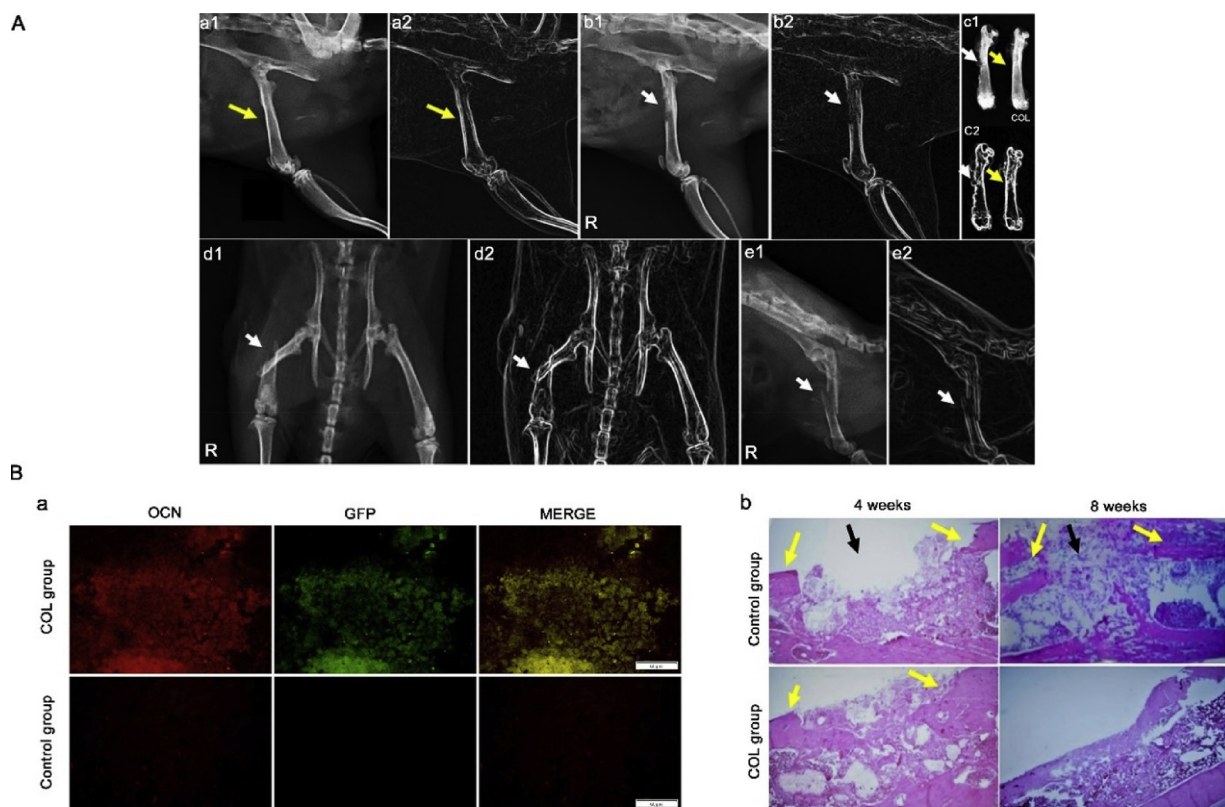


Fig. 8. Evaluation of the healing process of the femoral defect. (A) X-ray results of bone healing after an induced unilateral cortical defect (a1) lateral view of the right femur showed healing at the defect 4 weeks post induction in the COL group (yellow arrow), (b1) revealed the presence of the still defect in the control group appeared as a radiolucent area in the diaphysis of the femur (white arrow), (c1) PM X-ray of the femur showed complete healing in the COL group (yellow arrow); while the control group showed incomplete healing appeared a s radiolucent defect at the diaphysis (white arrow). (d1) AP view of rat femur suffered from complete femoral fracture in the control group (white arrow), (e1) the same animal with different view (Lateral). a2, b2, c2, d2, and e2 are the same pictures of a1, b1, c1, d1, and e1 respectively, after processing with Image J software to clarify the extent of defect; (B) Histological assessment of the bone defect after 4 and 8 weeks post transplantation. MEF transduced with LMP-3, c-Myc, and Oct4 were transplanted into the induced bone defect using Matrigel as a scaffold (COL group); while in the control group only Matrigel was introduced into the defect. Rats were killed at 4&8 weeks post transplantation. a) GFP-transduced cells were detected in the cryosections from the transplantation site in COL group (Original: 40X). b) histopathological sections of the femur in both control and COL groups stained with H&E. Yellow arrows showed the rim of the defect, and black arrows showed the defect area (Original: 40X). c-Myc + Oct4 + hLMP-3 (COL). (For interpretation of the references to colour in this figure legend, the reader is referred to the web version of this article.)

treatment in the future. We can conclude that direct reprogramming is an efficient therapeutic technique in the field of orthopedic especially in the difficult cases. More research should be conducted to improve the transcription factors, delivery method, cell used, and the scaffold materials.

Acknowledgments

The authors would like to thank the members of surgery department, Animal Hospital in Yangzhou University for their help in the surgical experiments. This study was funded by National Natural Science Foundation of China, Grant/Award Numbers: 31472087, 31572390; College Students' innovation and entrepreneurship training program, Grant/Award Number: Yangzhou University No. ×20170702; the Project Funded by the Priority Academic Program Development of Jiangsu Higher Education Institutions for funding the study; key research and development program, Grant/Award Number: 2017YFE0108000; High level talents Q7 support program of Yangzhou University.

References

Ambrosetti, D., Holmes, G., Mansukhani, A., Basilico, C., 2008. Fibroblast growth factor signaling uses multiple mechanisms to inhibit Wnt-induced transcription in osteoblasts. *Mol. Cell. Biol.* 28 (15), 4759–4771.

Barba, M., Pirozzi, F., Saulnier, N., Vitali, T., Natale, M.T., Logroscino, G., Robbins, P.D.,

Gambotto, A., Neri, G., Michetti, F., 2012. Lim mineralization protein 3 induces the osteogenic differentiation of human amniotic fluid stromal cells through Kruppel-like factor-4 downregulation and further bone-specific gene expression. *Biomed Res. Int.* 2012.

Boden, S.D., Liu, Y., Hair, G.A., Helms, J.A., Hu, D., Racine, M., Nanes, M.S., Titus, L., 1998. LMP-1, a LIM-domain protein, mediates BMP-6 effects on bone formation. *Endocrinology* 139 (12), 5125–5134.

Boden, S.D., Titus, L., Hair, G., Liu, Y., Viggeswarapu, M., Nanes, M.S., Baranowski, C., 1999. Spine-Lumbar Spine Fusion by Local Gene Therapy with a cDNA Encoding a Novel Osteoinductive Protein (LMP-1). *Adv. Orthop. Surg.* 22 (6) 302-302.

Caplan, A.I., 2007. Adult mesenchymal stem cells for tissue engineering versus regenerative medicine. *J. Cell. Physiol.* 213 (2), 341–347.

Costa-Almeida, R., Soares, R., Granja, P.L., 2018. Fibroblasts as maestros orchestrating tissue regeneration. *J. Tissue Eng. Regen. Med.* 12 (1), 240–251.

Cristofalo, V.J., Allen, R.G., Pignolo, R.J., Martin, B.G., Beck, J.C., 1998. Relationship between donor age and the replicative lifespan of human cells in culture: a re-evaluation. *Proc. Natl. Acad. Sci.* 95 (18), 10614–10619.

Ding, D., Xu, H., Liang, Q., Xu, L., Zhao, Y., Wang, Y., 2012. Over-expression of Sox2 in C3H10T1/2 cells inhibits osteoblast differentiation through Wnt and MAPK signalling pathways. *Int. Orthop.* 36 (5), 1087–1094.

Efe, J.A., Hilcove, S., Kim, J., Zhou, H., Ouyang, K., Wang, G., Chen, J., Ding, S., 2011. Conversion of mouse fibroblasts into cardiomyocytes using a direct reprogramming strategy. *Nat. Cell Biol.* 13 (3), 215.

El-Sayed, A.K., Zhang, Z., Zhang, L., Liu, Z., Abbott, L.C., Zhang, Y., Li, B., 2014. Pluripotent state induction in mouse embryonic fibroblast using mRNAs of reprogramming factors. *Int. J. Mol. Sci.* 15 (12), 21840–21864.

Ellis, P., Fagan, B.M., Magness, S.T., Hutton, S., Taranova, O., Hayashi, S., McMahon, A., Rao, M., Pevny, L., 2004. SOX2, a persistent marker for multipotential neural stem cells derived from embryonic stem cells, the embryo or the adult. *Dev. Neurosci.* 26 (2-4), 148–165.

Evans, C.H., Ghivizzani, S.C., Robbins, P.D., 2009. Orthopedic gene therapy in 2008. *Mol. Ther.* 17 (2), 231–244.

Evans, P.M., Liu, C., 2008. Roles of Kruppel-like factor 4 in normal homeostasis, cancer

and stem cells. *Acta biochimica et biophysica Sinica* 40 (7), 554–564.

Hall, L., Clarke, K., Trim, C., 2001. In: Saunders, W.B. (Ed.), *Anaesthesia of Birds, Laboratory Animals and Wild Animals*, 10th ed. Harcourt Publishers Limited, England.

Han, D.W., Tapia, N., Hermann, A., Hemmer, K., Höing, S., Araúzo-Bravo, M.J., Zaehres, H., Wu, G., Frank, S., Moritz, S., 2012. Direct reprogramming of fibroblasts into neural stem cells by defined factors. *Cell Stem Cell* 10 (4), 465–472.

Hiramatsu, K., Sasagawa, S., Outani, H., Nakagawa, K., Yoshikawa, H., Tsumaki, N., 2011. Generation of hyaline cartilaginous tissue from mouse adult dermal fibroblast culture by defined factors. *J. Clin. Invest.* 121 (2), 640–657.

Hjortholm, N., Jaddini, E., Hahaburda, K., Snarski, E., 2013. Strategies of pain reduction during the bone marrow biopsy. *Ann. Hematol.* 92 (2), 145–149.

Huang, P., He, Z., Ji, S., Sun, H., Xiang, D., Liu, C., Hu, Y., Wang, X., Hui, L., 2011. Induction of functional hepatocyte-like cells from mouse fibroblasts by defined factors. *Nature* 475 (7356), 386.

Huschtscha, L.I., Napier, C.E., Noble, J.R., Bower, K., Au, A.Y.M., Campbell, H.G., Braithwaite, A.W., Reddel, R.R., 2012. Enhanced isolation of fibroblasts from human skin explants. *Biotechniques* 53 (4), 239.

Ieda, M., Fu, J.-D., Delgado-Olguin, P., Vedantham, V., Hayashi, Y., Bruneau, B.G., Srivastava, D., 2010. Direct reprogramming of fibroblasts into functional cardiomyocytes by defined factors. *Cell* 142 (3), 375–386.

Ishihara, A., 2009. Gene and Cell-based BMP-2 and -6 Gene Therapy for Equine Bone Regeneration, Electronic PhD Dissertation in Veterinary Biosciences. Ohio State University.

Jayakumar, P., Di Silvio, L., 2010. Osteoblasts in bone tissue engineering. *Proc. Inst. Mech. Eng. Part H: Eng. Med.* 224 (12), 1415–1440.

Kim, J.H., Kim, K., Youn, B.U., Lee, J., Kim, I., Shin, H.-I., Akiyama, H., Choi, Y., Kim, N., 2014. Krüppel-like factor 4 attenuates osteoblast formation, function, and cross talk with osteoclasts. *J. Cell Biol.* 204 (6), 1063–1074.

Kim, M., Kim, C., Choi, Y.S., Kim, M., Park, C., Suh, Y., 2012. Age-related alterations in mesenchymal stem cells related to shift in differentiation from osteogenic to adipogenic potential: implication to age-associated bone diseases and defects. *Mech. Ageing Dev.* 133 (5), 215–225.

Kim, Y.H., Cha, S.M., Naidu, S., Hwang, W.J., 2011. Analysis of postoperative complications for superficial liposuction: a review of 2398 cases. *Plast. Reconstr. Surg.* 127 (2), 863–871.

Lattanzi, W., Barba, M., Novegno, F., Massimi, L., Tesori, V., Tamburini, G., Galgano, S., Bernardini, C., Caldarelli, M., Michetti, F., 2013. Lim mineralization protein is involved in the premature calvarial ossification in sporadic craniostostoses. *Bone* 52 (1), 474–484.

Lattanzi, W., Parrilla, C., Fetoni, A., Logroscino, G., Straface, G., Pecorini, G., Stigliano, E., Tampieri, A., Bedini, R., Pecci, R., 2008. Ex vivo-transduced autologous skin fibroblasts expressing human Lim mineralization protein-3 efficiently form new bone in animal models. *Gene Ther.* 15 (19), 1330.

Li, C.-S., Yang, P., Ting, K., Aghaloo, T., Lee, S., Zhang, Y., Khalilnejad, K., Murphy, M.C., Pan, H.C., Zhang, X., 2016. Fibromodulin reprogrammed cells: A novel cell source for bone regeneration. *Biomaterials* 83, 194–206.

Li, J.-Y., Christophersen, N.S., Hall, V., Soulet, D., Brundin, P., 2008. Critical issues of clinical human embryonic stem cell therapy for brain repair. *Trends Neurosci.* 31 (3), 146–153.

Li, Y., Wang, Y., Yu, J., Ma, Z., Bai, Q., Wu, X., Bao, P., Li, L., Ma, D., Liu, J., 2017. Direct conversion of human fibroblasts into osteoblasts and osteocytes with small molecules and a single factor, Runx2. *bioRxiv* 127480.

Lin, Z., 2010. The Function and Regulation of LIM Domain Mineralization Protein (LMP) in Periodontal Ligament Progenitor Cells, Electronic PhD Dissertation in Oral Health Science. University of Michigan.

Lin, Z., Rios, H.F., Park, C.-H., Taut, A.D., Jin, Q., Sugai, J.V., Robbins, P.D., Giannobile, W.V., 2013. LIM domain protein-3 (LMP3) cooperates with BMP7 to promote tissue regeneration by ligament progenitor cells. *Gene Ther.* 20 (1).

Liú, Y., Hair, G.A., Boden, S.D., Viggesswarupu, M., Titus, L., 2002. Overexpressed LIM mineralization proteins do not require LIM domains to induce bone. *J. Bone Miner. Res.* 17 (3), 406–414.

Liú, Y., Wu, J., Zhu, Y., Han, J., 2014. Therapeutic application of mesenchymal stem cells in bone and joint diseases. *Clin. Exp. Med.* 14 (1), 13–24.

Mansukhani, A., Ambrosetti, D., Holmes, G., Cornivelli, L., Basilio, C., 2005. Sox2 induction by FGF and FGFR2 activating mutations inhibits Wnt signaling and osteoblast differentiation. *J. Cell Biol.* 168 (7), 1065–1076.

Michikami, I., Fukushima, T., Tanaka, M., Egusa, H., Maeda, Y., Ooshima, T., Wakisaka, S., Abe, M., 2012. Krüppel-like factor 4 regulates membranous and endochondral ossification. *Exp. Cell Res.* 318 (4), 311–325.

Minamide, A., Boden, S.D., Viggesswarupu, M., Hair, G.A., Oliver, C., Titus, L., 2003. Mechanism of bone formation with gene transfer of the cDNA encoding for the intracellular protein LMP-1. *JBJS* 85 (6), 1030–1039.

Mizoshiri, N., Kishida, T., Yamamoto, K., Shirai, T., Terauchi, R., Tsuchida, S., Mori, Y., Ejima, A., Sato, Y., Arai, Y., 2015. Transduction of Oct6 or Oct9 gene concomitant with Myc family gene induced osteoblast-like phenotypic conversion in normal human fibroblasts. *Biochem. Biophys. Res. Commun.* 467 (4), 1110–1116.

Nakagawa, M., Koyanagi, M., Tanabe, K., Takahashi, K., Ichisaka, T., Aoi, T., Okita, K., Mochiduki, Y., Takizawa, N., Yamanaka, S., 2008. Generation of induced pluripotent stem cells without Myc from mouse and human fibroblasts. *Nat. Biotechnol.* 26 (1), 101.

Okita, K., Yamanaka, S., 2011. Induced pluripotent stem cells: opportunities and challenges. *Philos. Trans. R. Soc. B: Biol. Sci.* 366 (1575), 2198–2207.

Outani, H., Okada, M., Yamashita, A., Nakagawa, K., Yoshikawa, H., Tsumaki, N., 2013. Direct induction of chondrogenic cells from human dermal fibroblast culture by defined factors. *PLoS One* 8 (10).

Pang, Z.P., Yang, N., Vierbuchen, T., Ostermeier, A., Fuentes, D.R., Yang, T.Q., Citri, A., Sebastian, V., Marro, S., Südhof, T.C., 2011. Induction of human neuronal cells by defined transcription factors. *Nature* 476 (7359), 220.

Park, M.S., Kim, S.S., Cho, S.W., Choi, C.Y., Kim, B.S., 2006. Enhancement of the osteogenic efficacy of osteoblast transplantation by the sustained delivery of basic fibroblast growth factor. *J. Biomed. Mater. Res. Part B Appl. Biomater.* 79 (2), 353–359.

Park, S.B., Seo, K.W., So, A.Y., Seo, M.S., Yu, K.R., Kang, S.K., Kang, K.S., 2012. SOX2 has a crucial role in the lineage determination and proliferation of mesenchymal stem cells through Dickkopf-1 and c-MYC. *Cell Death Differ.* 19 (3), 534.

Pevny, L.H., Nicolis, S.K., 2010. Sox2 roles in neural stem cells. *Int. J. Biochem. Cell Biol.* 42 (3), 421–424.

Pola, E., Gao, W., Zhou, Y., Pola, R., Lattanzi, W., Sfeir, C., Gambotto, A., Robbins, P.D., 2004. Efficient bone formation by gene transfer of human LIM mineralization protein-3. *Gene Ther.* 11 (8), 683.

Qian, L., Huang, Y., Spencer, C.I., Foley, A., Vedantham, V., Liu, L., Conway, S.J., Fu, J.-d., Srivastava, D., 2012. In vivo reprogramming of murine cardiac fibroblasts into induced cardiomyocytes. *Nature* 485 (7400), 593.

Salgia, R., Li, J.-L., Lo, S.H., Brunckhorst, B., Kansas, G.S., Sobhany, E.S., Sun, Y., Pisic, E., Hallek, M., Ernst, T., 1995. Molecular cloning of human paxillin, a focal adhesion protein phosphorylated by P210BCR/ABL. *J. Biol. Chem.* 270 (10), 5039–5047.

Schindelin, J., Arganda-Carreras, I., Frise, E., Kaynig, V., Longair, M., Pietzsch, T., Preibisch, S., Rueden, C., Saalfeld, S., Schmid, B., 2012. Fiji: an open-source platform for biological-image analysis. *Nat. Methods* 9 (7), 676.

Schönitzer, V., Wirtz, R., Ulrich, V., Berger, T., Karl, A., Mutschler, W., Schieker, M., Böcker, W., 2014. Sox2 is a potent inhibitor of osteogenic and adipogenic differentiation in human mesenchymal stem cells. *Cell. Reprogram. (Formerly Cloning and Stem Cells)* 16 (5), 355–365.

Shu, J., Wu, C., Wu, Y., Li, Z., Shao, S., Zhao, W., Tang, X., Yang, H., Shen, L., Zuo, X., 2013. Induction of pluripotency in mouse somatic cells with lineage specifiers. *Cell* 153 (5), 963–975.

Sommar, P., Junker, J.P.E., Strandenes, E., Ness, C., Hansson, T., Johnson, H., Kratz, G., 2013. Osteogenically-induced human dermal fibroblasts as a tool to regenerate bone. *J. Plast. Surg. Hand Surg.* 47 (1), 8–13.

Szabo, E., Rampalli, S., Risueno, R.M., Schnerch, A., Mitchell, R., Fiebig-Comyn, A., Levadoux-Martin, M., Bhatia, M., 2010. Direct conversion of human fibroblasts to multilineage blood progenitors. *Nature* 468 (7323), 521.

Takahashi, K., Tanabe, K., Ohnuki, M., Narita, M., Ichisaka, T., Tomoda, K., Yamanaka, S., 2007. Induction of pluripotent stem cells from adult human fibroblasts by defined factors. *Cell* 131 (5), 861–872.

Takahashi, K., Yamanaka, S., 2006. Induction of pluripotent stem cells from mouse embryonic and adult fibroblast cultures by defined factors. *Cell* 126 (4), 663–676.

Thier, M., Wörsdörfer, P., Lakes, Y.B., Gorris, R., Herms, S., Opitz, T., Seiferling, D., Quandell, T., Hoffmann, P., Nöthen, M.M., 2012. Direct conversion of fibroblasts into stably expandable neural stem cells. *Cell Stem Cell* 10 (4), 473–479.

Ullah, M., Sittinger, M., Ringe, J., 2014. Transdifferentiation of adipogenically differentiated cells into osteogenically or chondrogenically differentiated cells: phenotype switching via dedifferentiation. *Int. J. Biochem. Cell Biol.* 46, 124–137.

Vierbuchen, T., Ostermeier, A., Pang, Z.P., Kokubu, Y., Südhof, T.C., Wernig, M., 2010. Direct conversion of fibroblasts to functional neurons by defined factors. *Nature* 463 (7284), 1035.

Walia, B., Satija, N., Tripathi, R.P., Gangenahalli, G.U., 2012. Induced pluripotent stem cells: fundamentals and applications of the reprogramming process and its ramifications on regenerative medicine. *Stem Cell Rev. Rep.* 8 (1), 100–115.

Wang, Y., Wu, M.-H., Cheung, M.P.L., Sham, M.H., Akiyama, H., Chan, D., Cheah, K.S., Cheung, M., 2017a. Reprogramming of dermal fibroblasts into osteo-chondrogenic cells with elevated osteogenic potency by defined transcription factors. *Stem Cell Rep.* 8 (6), 1587–1599.

Wang, Y., Zhang, X., Shao, J., Liu, H., Liu, X., Luo, E., 2017b. Adiponectin regulates BMSC osteogenic differentiation and osteogenesis through the Wnt/β-catenin pathway. *Sci. Rep.* 7 (1), 3652.

Yamamoto, K., Kishida, T., Nakai, K., Sato, Y., Kotani, S.-i., Nishizawa, Y., Yamamoto, T., Kanamura, N., Mazda, O., 2018. Direct phenotypic conversion of human fibroblasts into functional osteoblasts triggered by a blockade of the transforming growth factor-β signal. *Sci. Rep.* 8 (1), 8463.

Yamamoto, K., Kishida, T., Sato, Y., Nishioka, K., Ejima, A., Fujiwara, H., Kubo, T., Yamamoto, T., Kanamura, N., Mazda, O., 2015. Direct conversion of human fibroblasts into functional osteoblasts by defined factors. *Proc. Natl. Acad. Sci.* 112 (19), 6152–6157.

Yamanaka, S., 2007. Strategies and new developments in the generation of patient-specific pluripotent stem cells. *Cell Stem Cell* 1 (1), 39–49.

Yoon, S.T., Boden, S.D., 2004. Spine fusion by gene therapy. *Gene Ther.* 11 (4), 360.

Yoon, S.T., Park, J.S., Kim, K.S., Li, J., Attallah-Wasif, E.S., Hutton, W.C., Boden, S.D., 2004. ISSLS prize winner: LMP-1 upregulates intervertebral disc cell production of proteoglycans and BMPs in vitro and in vivo. *Spine* 29 (23), 2603–2611.

Young, D.W., Pratap, J., Javed, A., Weiner, B., Ohkawa, Y., Van Wijnen, A., Montecino, M., Stein, G.S., Stein, J.L., Imbalzano, A.N., 2005. SWI/SNF chromatin remodeling complex is obligatory for BMP2-induced, Runx2-dependent skeletal gene expression that controls osteoblast differentiation. *J. Cell. Biochem.* 94 (4), 720–730.

Yu, B., He, Z.-Y., You, P., Han, Q.-W., Xiang, D., Chen, F., Wang, M.-J., Liu, C.-C., Lin, X.-W., Borjigin, U., 2013. Reprogramming fibroblasts into bipotential hepatic stem cells by defined factors. *Cell Stem Cell* 13 (3), 328–340.

Zhao, T., Zhang, Z.-N., Rong, Z., Xu, Y., 2011. Immunogenicity of induced pluripotent stem cells. *Nature* 474 (7350), 212.